Limit State Design Framework for Geosynthetic-Reinforced Soil Structures

Dov Leshchinsky, Ph.D.[a], Ben Leshchinsky, Ph.D.[b], P.E. and Ora Leshchinsky, P.E.[a]

NOTE: The following is a prepublication, unedited manuscript. It explains the methodology for finding the distribution of force in reinforcement layers to ensure a prescribed stability at each location. You can obtain a copy of the published paper from Elsevier at: http://www.sciencedirect.com/science/article/pii/S0266114417301036 . If you need a copy for educational purposes, please contact Dov Leshchinsky at dov@UDel.edu .

The published reference is cited as: Dov Leshchinsky, Ben Leshchinsky, Ora Leshchinsky, "Limit state design framework for geosynthetic-reinforced soil structures," *Geotextiles and Geomembranes*, Volume 45, Issue 6, 2017, Pages 642-652, ISSN 0266-1144, https://doi.org/10.1016/j.geotexmem.2017.08.005.

[a]Principal, ADAMA Engineering, Inc.,12042 SE Sunnyside Road, Suite 711, Clackamas, OR 97015, USA
[b]Corresponding Author, Dept. of Forest Eng., Res. and Mgmt., Oregon State University, 280 Peavy Hall, Corvallis, OR 97331, USA, +1-541-737-8873, ben.leshchinsky@oregonstate.edu

Abstract

Conventional design of geosynthetic-reinforced soil structures is divided into two categories, walls and slopes, based on the batter of its facing system. Internal stability, characterized as sufficient reinforcement anchoring and strength, is performed using earth pressure-based design criteria for reinforced walls while reinforced slopes are founded on limit equilibrium (LE) based slope stability analyses. LE analyses are also used to assess the global or compound stability of both types of structures, accounting for the geometry of the reinforced, retained and foundation soils. The application of LE-based methods typically results in determination of a slip surface corresponding to the lowest attained Safety Factor (*SF*), known as the Factor of Safety (*Fs*); however, it yields little information about reinforcement loading or connection load. In this study, use of the analyzed spatial distribution of slip surfaces known as a *Safety Map*, is modified to discretize reinforcement layers and the required tensions to attain a prescribed constant *Fs* at any location in the reinforced soil mass. This modified framework, implemented through an iterative, *top-down* procedure of LE slope stability analyses originating from the crest of a reinforced structure and exiting at progressively lower elevations on the facing, enables the determination of a *Tension Map* that illustrates the required distribution of reinforcement tension to attain a prescribed limit state of equilibrium. This tension map is directly constrained by a pullout capacity envelope at both the rear and front of each reinforcement layer, providing a unified, LE-based approach towards assessing an optimal selection of mutually dependent strength *and* layout of the reinforcement. To illustrate the utility of the Limit State framework, a series of instructive examples are presented. The results demonstrate the effects of

facing elements, closely-spaced reinforcements, secondary reinforcement layers, and is compared to conventional design approaches.

Keywords: *Geosynthetics; MSE walls; Reinforced Steep Slopes, Limit Equilibrium, Slope Stability*

Introduction

Geosynthetics have been widely used as an economical means of soil reinforcement in both walls and slopes in recent years. Current design of reinforced soil structures in the United States distinguishes between slopes and walls using the batter angle as a criterion. When the inclination of the face is equal to or less than 20°, the structure is defined as a reinforced wall. Conversely, when the batter is greater than 20°, it is defined as a reinforced slope (Berg et al. 2009, AASHTO 2012, NCMA 1997). These different soil structures employ different design methodologies, potentially leading to significantly different outcomes. This inclination-based design distinction simplifies the design of walls, requiring a synthesis of basic, semi-empirical calculations to evaluate internal and external stability (with the exception for global or compound stability). While the aforementioned approach to wall design results in safe structures, it is not consistent with traditional and well-established geotechnical design of similar structures that are ‘arbitrarily’ differentiated by batter: slopes. Evaluating design of reinforced slopes and walls can be considered as a subset of slope stability that considers traditional slope problem with the added forces of elements such as

reinforcements and facing, constructed over a foundation soil (Leshchinsky and Reinschmidt, 1985, Leshchinsky and Boedeker 1989, Duncan and Wright 1991, Leshchinsky et al. 1995). In these analyses, slope inclination (or batter) is just a typical design variable, not a delineator of calculation convenience. Use of a unified approach in limit state design of reinforced 'walls' and 'slopes' reduces confusion related to the mechanics behind design. It offers consistency regardless of the structure being considered thus lessens the level of judgment and subjectivity associated with designs, especially of structures having complex geometries and non-uniform soil profiles – both realistic scenarios for reinforced soil structures.

Limit equilibrium (LE) analysis has been used successfully in the design of complex and critical structures (e.g., tall dams) for many decades. The LE formulation requires governing assumptions in statics and/or geometry of failure (i.e. kinematics). Hence, there are a variety of LE methods, each of which is based on different assumptions (Duncan 1996). The simplicity and demonstrated performance of LE approaches have cemented it as a mainstream design tool in the US.

Limit state analysis, including LE, assumes that the *design* strength of the soil in consideration is mobilized. The degree of mobilization (or utilization) signifies the margin or factor of safety, *Fs*. Reinforcement is installed in slopes that otherwise are inherently unstable. That is, at an actual limit state the *design* strength of the soil is fully mobilized (i.e. $Fs=1.0$) and stability hinges upon the mobilized tensile resistance of the reinforcement. At that state, design should ensure that the long-term strength of the reinforcement will be available throughout the reinforcement (e.g., Leshchinsky et al. 2016). An implicit assumption in this concept is that the reinforcement will not rupture as

85 the soil deforms during mobilization of its strength (e.g., Liu 2016). Often this
86 phenomenon is referred to as compatibility. Geosynthetic reinforcements are generally
87 ductile ('extensible'), capable of developing substantial strain (typically >8%) before
88 rupture. Such planar strains are much larger than those needed for granular compacted
89 backfill to mobilize its strength (i.e., to form an 'active' mass). From this perspective,
90 combined with experimental and numerical investigations reviewed by Leshchinsky et
91 al. (2016), the limit state concept and LE in particular are suitable for design of
92 geosynthetic reinforced slopes/walls. This assertion is supported by the performance of
93 numerous reinforced slopes designed and constructed over the past three decades as
94 reported in proceedings of many relevant conferences. However, reported experimental
95 and numerical confirmation of relatively brittle (i.e., 'inextensible') reinforcement,
96 designed based on limit state analysis, is scarce (Leshchinsky et al. 2016). Hence, the
97 question of compatibility of inextensible reinforcement in the context of limit state still
98 remains. Consequently, the scope of this study is limited to extensible reinforcement
99 that exhibits ductile behavior relative to the soils involved.

100 Note that while LE is employed to analyze the limit state in this study, one may
101 use alternative approaches, such as *limit analysis*, LA, of plasticity (Rowe and Ho 1992,
102 Xie and Leshchinsky 2015, Smith and Tatari 2016). Furthermore, numerical methods
103 that can deal with limit state, such as finite element (FE) and finite difference (FD)
104 analyses may also be implemented within the context of the framework (Leshchinsky
105 and Han 2004, Leshchinsky and Vulova 2001, Mohamed et al. 2014). However, while
106 continuum mechanics-based numerical methods are insightful, implementation of these
107 approaches in ordinary design may add unnecessary complexity.

Safety Map

Although various LE stability analyses have been developed for design of reinforced slopes (e.g. Duncan and Wright 2005), few discuss specific, yet practical details associated with mobilized tensile resistance along reinforcements. Baker and Klein (2004a, 2004b) modified the top-down approach by Leshchinsky (1992) using planar surfaces. Han and Leshchinsky (2006) used an alternative approach to Baker and Klein (2004a) considering more efficient load distribution among reinforcement layers. Leshchinsky et al. (2014) used log spiral surfaces to calculate the required tensile resistance along the reinforcement, including at the connection to the facing, providing considerations for a LE design framework. The use of log spiral enabled examination of non-vertical reinforced slopes as planar surfaces then become less critical. Modification and generalization of this framework to deal with realistic problems is presented in the *Tension Map* section followed by a section of *Illustrative Examples*.

It is noted that stability of reinforced soil structures is a subset of slope stability problems and some design codes allow for LE-based design of such structures (Leshchinsky et al., 2016). FHWA and AASHTO require LE design of reinforced *slopes*, arbitrarily defining it as having a maximum inclination of 70°, while requiring LE assessment of global stability of reinforced *walls* (i.e., inclination $\geq$70°) as a final design step. LE analysis is recognized by FHWA and AASHTO as a legitimate strength limit state design tool; however, its implementation is lacking.

Use of LE for slope stability (reinforced or unreinforced) requires iteration of multiple slip surfaces until a failure surface that corresponds to a critical, minimum *Fs* is determined. One means of demonstrating this process graphically is the *safety map* methodology (Baker and Leshchinsky 2001). In addition to illustrating the relative spatial stability of a given geotechnical problem, the distribution of shear surfaces can inform the relative tensile mobilization of reinforcements in a reinforced soil structure using an LE approach. The safety map is used within this study to select a satisfactory layout and strength of reinforcements. It is presented through an instructive simple example

The safety map, in context of reinforced soil, indicates whether the assumed strength and length of reinforcement produces adequate stability. The specified strength of reinforcement along its length is illustrated in Fig. 1. Note that at any location along the reinforcement, its strength is limited by either its long-term intrinsic rupture strength or its pullout resistance, whichever value is smaller. Pullout resistance is a function of the overburden pressure, reinforcement anchorage length, and reinforcement-soil interface properties. At the front end of the reinforcement, pullout is superimposed on a boundary value which is the long-term strength of the connection when moving from the front of the reinforcement into the backfill soil. That is, the value at the boundary is at the connection and the reinforcement there can mobilize strength that is limited by the connector capacity or the reinforcement long-term strength, whichever is smaller. At the back end of the reinforcement, the boundary value is zero and pullout is governed only by the anchorage and frictional interaction with the overburden fill. Consequently, the basic premise of conventional LE analyses is consideration of the long-term tensile resistance of the reinforcement, including at the connection, rather than calculating the

actual load values for a given factor of safety. It is noted that for simplicity the pullout resistance shown in Fig. 1 varies linearly, thus reflecting a simple geometry with zero batter and a horizontal crest. For more complex boundary conditions, the pullout resistance distribution will not be linear, as discussed in the Illustrative Examples section.

The factor of safety, *Fs*, used in current LE methods is related to the soil shear strength. It signifies the value by which the soil strength should be reduced to attain equilibrium at a limit state. It means that the reciprocal value of *Fs* (i.e., *1/Fs*) signifies the average level of mobilization of the soil strength along a surface of shear. The *safety factor*, *SF*, is determined the same way as *Fs*, but is representative of the mobilized shear strength for any analyzed surface within the soil mass, even if it is not the critical slip surface. Specifically, for each analyzed potential slip surface there is an associated *safety factor*, *SF*, and the *factor of safety*, *Fs*, corresponds to the lowest *SF*:

$$Fs = \min(SF) \tag{1}$$

The most likely (i.e., the critical) slip surface is associated with *Fs*. In computerized slope stability analysis, thousands of slip surfaces may be analyzed, each producing a certain safety factor, *SF*. Conventionally, all *SF* are discarded except for the lowest value corresponding to *Fs*. The safety map presents the distribution of *SF* to provide a diagnostic tool for assessing the spatial distribution of stability throughout the slope. It is noted that introduction of the safety map was initially conducted mathematically (Baker and Leshchinsky 2001). That is, the contour lines of *SF* associated with numerous analyzed potential slip surfaces were mathematically proven to not intersect

with one another, making the concept of safety map physically valid. Mathematical verity aside, the practical implications of the safety map in the context of current LE design of reinforced soil is best demonstrated through an example problem.

Consider a simple reinforced wall, H=6 m tall having a batter of ω=8^o. Reinforcement spacing (S_v) is 0.6 m with a bottom layer 0.3 above the foundation soil and the top layer is 0.3 m below the horizontal crest. The length of reinforcement, L, follows FHWA (Berg et al., 2009) recommendations of L/H=0.7; i.e., L= 4.20 m – Fig. 2b. The reinforced, retained, and foundation soils have unit weight, γ, of 22, 20, and 18 kN/m^3, respectively, and internal angle of friction, ϕ, of 34, 30, and 28 degrees, respectively. Possible cohesion of any soil is ignored. The selected geosynthetic has long-term design strength, T_{LTDS}, of 16 kN/m. The long-term strength of the connection is assumed to be equal to T_{LTDS}. Pullout resistance is commonly calculated by integrating the following elemental value:

$$dP_r = R_c\, \sigma\, C_i\, \tan\phi\, dx \qquad (2)$$

where dP_r is the pullout resistance over length dx, σ is the average overburden pressure above dx, commonly taken as equal to γZ where Z is the vertical distance to the soil surface above dx (if induced stress due to vertical dead load surcharge acts over dx, its value is added to σ), ϕ is the friction angle of the soil along which dx is embedded, R_c is the coverage ratio (usually 100% with geosynthetics), and C_i is the experimentally-determined interaction coefficient. The available pullout resistance at any point along a reinforcement layer results from integration of Eq. 2 from its end to the point of interest. It is common to reduce the calculated pullout resistance by a factor of safety, Fs-po, of

1.5 for a given layer. For the example problem, the following values were considered in calculating pullout: C_i=0.64, R_c=1.0, and *Fs-po*=1.50.

Fig. 2 presents the free body diagram and safety map generated for the example problem using Bishop's Method considering circular slip surfaces, where SF is (Leshchinsky et al., 2016):

$$SF = \frac{\sum\left[\frac{c'_j \Delta x_j + (W_j + Q_{vj} - u_j \Delta x_j) tan\phi'_j}{cos\alpha_j + (sin\alpha_j tan\phi'_j)/F}\right]}{\sum (W_j + Q_{vj}) sin\alpha_j + \frac{Q_{hj} d_j}{R} - T_i R_c cos\alpha_j} \quad (3)$$

Where c_j is cohesion, Δx is the width of a given slice, W_j is the weight of a given slice, Q_{vj} is a vertical surcharge, Q_{hj} is a vertical surcharge, u_j is a boundary neutral force, ϕ' is the internal angle of friction, α_j is the inclination of the slice shear plane, R is the failure surface radius, T_i is the tensile force of a reinforcement and R_c is coverage ratio. For the given problem, *Fs*=1.30, associated with a circle that extends through the retained soil, intersects the rear portion of the lower reinforcement layer and the reinforced soil, and emerges through the foundation soil. The critical circle alone does not indicate whether the design is efficient. Conversely, the safety map shows that the zone representative of spatial safety factors varying between 1.3 and 1.5 is expansive, especially within the reinforced soil zone, implying that the length and selected strength of reinforcement is efficient. Different layouts of reinforcement and/or different T_{LTDS} would have rendered different safety maps possibly indicating an under-designed or over-designed reinforced

slope. The safety map is an objective visual tool that facilitates an efficient selection of reinforcement layout.

Note that while using the safety map tool, the designer still needs to use a trial-and-error process to select adequate reinforcement properties and configuration. As is, the analysis does not explicitly produce the loads along each reinforcement layer and at each connection. The distribution of individual reinforcement load values, termed herein as the *tension map*, are the basics needed for rational and robust design of geosynthetic-reinforced soil structures. In current design, the safety map is employed to ensure an adequately stable system in a global sense. That is, some layers could be overstressed as local conditions may require higher strength than needed to satisfy global stability. However, as shown next, a special case of the safety map can serve as a basis for rationally determining a tension map in context of complex, yet realistic design considerations that include soil-reinforcement interaction along common interfaces, properties of soil layers, irregular reinforcement layout, facing units, and complex slope geometry. In a sense, this special case is a generalization of an analysis commonly known as ‘internal stability’.

Tension Map

The Tension Map illustrates the distribution of load along each reinforcement layer to ensure that a limit state defined by a prescribed safety factor is rendered. That is, rather than using the long term strength of each reinforcement as depicted in Fig. 1, the required reinforcement tension at the intersection of an analyzed slip surface is modified to produce a prescribed *SF* in the slip surface of concern. This implies that, within a numerical tolerance, failure is equally likely to occur along any analyzed slip

surface; i.e., for each analyzed slip surface the corresponding safety factor is *Fs=SF=constant*. From a design viewpoint, for each layer *i*, the Tension Map yields the maximum load in the reinforcement including its connection load: $T_{max\text{-}i}$ and $T_{o\text{-}i}$, respectively. For a selected layout, these values allow the designer to rationally select adequate reinforcements and connection specifications.

To implement the tension map solution with the inverse of the safety map, a *top-down procedure* must be employed. This procedure is characterized by analyzing multiple slip surfaces, initially emerging through the slope face near the crest, progressing downwards to the toe with added slip surfaces. This approach results in a computational scheme that enables assessment of loading throughout multiple layers of reinforcement that may account for redistribution of reinforcement loading for a given surface *and* compliance with a prescribed *SF=Fs=constant*. The ultimate product of this iterative process is the determination of a Tension Map. The generic steps implicit in the *top-down procedure* are described below and in Figure 3:

Top-down procedure

1. Develop a trial layout or arrangement of reinforcement layers; i.e., vertical spacing and length behind the face of the slope.

2. Generally, using a *top-down* arrangement going for reinforcement layers *i*=1, 2, 3…*n*, search and analyze failure surfaces that:

    a) Start at the crest and emerge at the slope face;
    b) robustly capture kinematics and spatial extent of potential failure;
    c) cross layers of reinforcement above, potentially extending into

the retained soil;

d) and do *not* yet cross the reinforcement layer below.

An illustrative schematic is provided in Figure 4. Start with layer *i*=1 considering surfaces emerging above layer *i*=2. For each failure surface evaluated in the search, adjust the mobilized reinforcement force so as to obtain the target *Fs*=*SF*. Once this is achieved, the resulting mobilized force, *T*, is assigned to at the reinforcement location where the slip surface intersects the reinforcement. This force indicates the tensile force that must be mobilized in a LE state for a prescribed *Fs*. Its location, relative to the rear of reinforcement layer *i*=1, indicates the embedded length over which pullout resistance behind the failure surface can develop. The calculated mobilized force cannot exceed rear end pullout resistance. *For surfaces emerging above the layer i=2, the uppermost layer, i*=1, *must have sufficient embedment length to develop the required pullout resistance since there are no layers to contribute resistance to ensure the stability prescribed by the target Fs*. For each location along the reinforcement, the *largest* mobilized force needed to obtain the target *Fs* for all failure surfaces crossing that point determines the required tensile force at that location. The completion of the stability analyses for this step produces the largest required force as a function of location along the length of the top reinforcement *i*=1.

3. Repeat Step 2 by searching from the top of the slope down to, but not crossing, the reinforcement *i*=3. *If the failure surface under consideration only crosses a single layer of reinforcement, the layer must have sufficient embedment length behind the*

surface to develop the required pullout resistance. If not, it must be lengthened. Surfaces crossing multiple layers of reinforcement are stabilized by the tension developed in, or shared by each reinforcement layer to obtain the target *Fs* on soil strength. The combined stabilizing resistance (e.g., moment when using Bishop's approach) provided by the reinforcement forces is distributed to each layer by initially assuming equal mobilization of force. *If the initial computational assumption of equal mobilization of force results in a layer's force that exceeds the available factored pullout resistance behind the surface, that layer is reassigned the maximum available factored pullout resistance. When this occurs, the tensions in the remaining layer(s) are increased assuming equal force mobilization such that the target Fs is achieved.* The mobilized tension determined for each layer of reinforcement at the location of intersection with a considered failure surface is then compared with mobilized tensions computed in previous failure surface analyses. Then, each of the reinforcement layers that are considered up to the present step are reassigned the highest mobilized tension *if* the current calculated tension exceeds those determined in previous steps. Forces are then *recalculated* or corrected in the stable remaining layers that have been crossed by the failure surface calculated before. This redistribution is done such that the combined stabilizing resistance provided by all of the reinforcement layers crossed by the failure surface under consideration produces the target *Fs*. For a given failure surface, this process may result in lower required forces in some layers compared to the *initial* assumption of equal force mobilization in all layers. As mentioned in Step 2, the largest reinforcing force needed to obtain the target *Fs* for all failure

surfaces crossing a given location along a reinforcement length determines the final required tensile force. Such redistribution of load amongst reinforcements ensures, within a numerical error tolerance, that for any slip surface emerging at the face of the slope, a limit state, manifested by a prescribed *Fs*, is rendered. At this stage, the mobilized tensile force distribution in layers 1 and 2, rendering a prescribed *Fs*, is ascertained considering surfaces emerging down to layer *i*=3, rear pullout factored resistance of layers 1 and 2, and reinforced and retained soil properties.

4. Repeat the processes described in Steps 2 and 3 until the toe elevation is reached. Now the required or mobilized force in each reinforcement layer considering rear pullout needed to render the same *Fs* throughout the reinforced soil mass is determined. Note that for uniform length of reinforcement, there could be zones within which no reinforcement is needed for a prescribed *Fs*. That is, such zones are inherently stable requiring negative reinforcement force to reduce the safety factor to the prescribed value *Fs*. Such cases are physically meaningless. Also note that surfaces emerging through the foundation and away from the toe should be considered in the scenario that the foundation material is not competent. However, in the presented study, consideration of foundation failure is ignored and a need for top-down assessment using deep-seated or foundation failures should be considered if indicated by global stability - see Stage II in design.

5. Determine connection loads, $T_{o\text{-}i}$, so that there is sufficient "front end" pullout capacity to enable the reinforcement to mobilize the required resistance, calculated in Steps 2-4, to produce the prescribed *Fs*. This is done by adjusting the front

pullout envelope so that the calculated required force in each layer is below this envelope. The amount of adjustment or shift from zero resistance at the slope is the minimum connection load at each elevation. Such adjustment is illustrated in the next section.

6. Based on $T_{max\text{-}i}$ and $T_{o\text{-}i}$, determine the minimum required long-term rupture strength of the reinforcement and the required connection capacity.

7. Adjust the lengths of reinforcement layers (Step 1) and repeat Steps 2 to 6 to achieve an economical design.

Visualization of the top-down procedure

The top-down process seeks the tensile load at discrete locations along a reinforcement length needed to produce the same *Fs* at any location within the reinforced mass. That is, it rationally establishes the baseline 'demand' for reinforcement force for a prescribed level of stability. Such a process leads to selection of reinforcement and connection that has the necessary long term capacity. It is a rational and robust alternative to lateral earth pressure design methods such as AASHTO.

To visualize the top-down process, consider the same problem presented in Fig. 2. Recall that the reinforced, retained, and foundation soils have unit weight, γ, of 22, 20, and 18 kN/m^3, respectively, and internal angle of friction, ϕ, of 34, 30, and 28 degrees, respectively. Note that in the presented example for the top-down approach, a typical factor of safety for pullout resistance, *Fs-po*=1.50, is applied in design. For the given relevant shear strength parameters, the factor of safety on soil strength,

352 *Fs*=*SF*=1.00 is specified. While one may use a larger target value of *Fs*, it is customary
353 (e.g., AASHTO 2012) to use the design value of soil strength *as is* when assessing the
354 maximum loads in the reinforcement and at the connection $T_{max\text{-}i}$ and $T_{o\text{-}i}$. Often this
355 calculation is done under a category known as 'internal stability'. Note that in Stage II
356 (discussed later) the reinforced system needs to have a global *Fs* having a minimum of
357 1.30.

358 For the layout in Fig. 2 (Step 1), Fig. 5a demonstrates the outcome of the
359 top-down approach (Steps 2 and 3) using Bishop's circular slip surfaces. The upper
360 portion of Fig. 5a shows the distribution of tensile load along the top layer, constrained
361 by its rear end pullout resistance. The load distribution for layer 2 is calculated
362 considering rear pullout of layer 1 resulting in an increased load in layer 2. That is,
363 there is some load shedding between the two layers. The transition for layers 1 to 3
364 demonstrates the decreasing influence of rear pullout resistance and the increased
365 load shedding between reinforcement layers. Once the basal layer (layer 10) is reached
366 (Step 4), the influence of rear end pullout is negligible (Fig. 5b). As seen in Figure 5b,
367 the upper 4 layers are affected by pullout. The "jagged", stepwise shape of the load
368 distributions stem from minor numerical inaccuracies associated with both the
369 discretization of reinforcement segments where loads are calculated and the solving of
370 nonlinear equation of discretized sliding mass.

371 After the top-down procedure is used to determine tension within the
372 reinforcements governed by rear pullout, Step 5 is performed, defined as a layer-by-
373 layer adjustment for front-end pullout (i.e. connection loading; see Figure 6). In this
374 example problem, the properties related to the reinforced soil are considered (see

details of Fig. 2b). The top-down procedure outlined in steps 2-4 yields the distribution of mobilized force in all reinforcement layers needed to produce a prescribed *Fs* while considering the rear end pullout constraints and load shedding amongst layers. These steps establish that a prescribed limit state exists along each analyzed surface emerging at or above the toe based on the premise that each reinforcement can indeed mobilize the calculated load. However, at this stage, this assumption must be validated at the front end. If the front end pullout does not provide sufficient resistance to enable the reinforcement to mobilize the force needed to ascertain *Fs* – see 4a and 4b for top and bottom layers, respectively – than the basic premise of the top-down LE analysis is not valid. As implied in Fig. 1, the front end pullout capacity envelope may begin at an existing boundary value, the connection capacity, which may render increased front end pullout resistance throughout the reinforcement length. Hence, to enable the required mobilized load calculated along each reinforcement layer, the front end pullout needs to be translated or shifted upwards until the pullout envelope is tangent to the calculated force distribution – see 4a (bottom) and 4b (right). While this shift enables the reinforcement to develop the calculated resistance, it rationally yields the connection load for each layer *i*, $T_{o\text{-}i}$, at a limit state. Determination of these connection loads provides the basic information for selecting a connector with sufficient minimum long-term strength, analogous to using $T_{max\text{-}i}$ in selecting a design geosynthetic.

Note in Fig. 5 that the maximum load in the reinforcement gets closer to the slope as lower layers are considered. Comparing Figs. 6a and 6b also demonstrate this behavior. However, front end pullout also increases with depth (see Figs. 6a and 6b), especially in steeper slopes as increased overburden increases frictional resistance.

Therefore, although $T_{max\text{-}i}$ gets closer to the slope, the required $T_{o\text{-}i}$ that enables mobilization of force in the reinforcement may not be high at lower layers - an important design consideration for slopes with higher batters.

It is interesting to note that the locus of $T_{max\text{-}i}$ does not necessarily lie on a singular trace of slip surface (a circle in Bishop's). For the current problem this locus is inferred by Fig. 5 and explicitly shown in Fig. 5 by black squares superimposed on a color-coded tension map. The top layer is heavily affected by rear pullout while lower layers are affected by compound failures. Closer and/or longer reinforcements may result in uniform mobilization of reinforcement occurring along a singular slip surface. Other configurations of reinforcement length and geometry may result in non-uniform mobilization of reinforcement strength, an aspect that cannot be addressed using conventional LE design approaches (Leshchinsky et al. 2016).

Design Aspects

The design framework follows two consecutive stages: the first stage using a top-down LE analysis and the second stage ensuring adequate reinforcement selection to resist a prescribed limit state.

Stage I:

Using the top-down approach, the maximum tension in each layer, $T_{max\text{-}i}$ (see also Fig. 5) and the connection load, $T_{o\text{-}i}$, at a limit state for a prescribed Fs=1.0 are generated (see Fig. 8). The values of $T_{o\text{-}i}$ between the top and the bottom layer exhibit a well-defined trend although there is some fluctuation due to minor numerical inaccuracy.

The two 'unfactored' or baseline distributions, $T_{max\text{-}i}$ and $T_{o\text{-}i}$, serve as the basis for selecting design reinforcements, connectors and facing elements. The ultimate strength of geosynthetic reinforcement, T_{ult}, is typically specified based on internal stability where Fs=1.0 (e.g., Berg et al. 2009) as:

$$T_{ult} \geq T_{max-i}\ RF_{id}\ RF_{d}\ RF_{cr}\ F_{s-g} \quad (4)$$

where RF_{id}, RF_{d}, and RF_{cr} are reduction factors for installation damage, durability, and creep, respectively, and $F_{s\text{-}g}$ is a factor of safety on the geosynthetic strength. For the simple problem used here, typically one type of geosynthetic is selected and hence, T_{max} for design is the maximum value considering all calculated values of $T_{max\text{-}i}$. The strength reduction factors depend on the polymer type, the manufacturing process, the backfill and construction, and the design lifespan of the structure. These values are well-established for most products and applications. The factor of safety on the geosynthetic strength, $F_{s\text{-}g,}$ is typically specified as 1.5. Note that there is little uncertainty about the long-term strength of the manmade geosynthetics. It seems that $F_{s\text{-}g}$ is related to uncertainty with conventional (e.g., AASHTO) 'internal stability' analysis. To be compatible with existing design practice, the same $F_{s\text{-}g}$ is used here in specifying geosynthetic with adequate ultimate strength.

Fig. 8 indicates that the maximum connection load is about 50% of the maximum force in the reinforcement. Hence, a connector with suitable long term strength can be specified using, for example, the procedure stated in AASHTO. Note that both $T_{max\text{-}i}$ and $T_{o\text{-}i}$ are affected by pullout resistance. Hence, the use of $Fs\text{-}po$=1.5, which in design decreases pullout substantially, indirectly increases the values of $T_{max\text{-}i}$ and $T_{o\text{-}i}$.

For illustrative purposes, Fig. 8 compares $T_{max\text{-}i}$ and $T_{o\text{-}i}$ as calculated by AASHTO and top-down LE. AASHTO uses a lateral earth pressure-based approach that is proportional to simple overburden pressure and reinforcement spacing. Since the reinforcement is equally spaced, $T_{max\text{-}i}$ increases linearly with depth. In top-down LE nearly all the layers are equally mobilized implying an efficient use of ductile reinforcement. If max($T_{max\text{-}i}$) is used to select a geosynthetic, AASHTO requires about twice the strength needed based on LE. AASHTO arbitrarily requires that $T_{o\text{-}i} = T_{max\text{-}i}$. Hence, except for the top layer, the difference in $T_{o\text{-}i}$ between LE and AASHTO increases substantially with depth.

Stage II:

Stage I provides a rational basis for the selection of geosynthetics and facing governed by maximum reinforcement loading and connection loads. This selection was done using a factor of safety, Fs=1.0, on the soil strength. That is, a reasonably conservative estimate of soil design strength yields the ultimate strength of the geosynthetic, T_{ult} as well as the basis for selecting connection specifications with adequate long-term strength. However, sound geotechnical design must ascertain that there is also adequate overall (global) stability of the reinforced structure. Conventional LE analysis is a common tool for such an assessment considering various slip surfaces including potential compound and foundation (deep-seated) failures. As demonstrated in Fig. 2, long term design strength of the geosynthetic, T_{LTDS}, is used in the stability analysis:

$$T_{LTDS} \geq \frac{T_{ult}}{RF_{id}\ RF_{d}\ RF_{cr}} \quad (5)$$

For the example problem, Fig. 5 or 8 indicate that in Stage I the max(T_{max}) is 11.28 kN/m. To find T_{ult} (Eq. 4), take $F_{s\text{-}g}$ =1.5 and, for demonstration of Stage II, assume that the multiplication of (RF_{id}, RF_{d}, RF_{cr})=2.0. Consequently, T_{ult} is 33.84 kN/m. Use Eq. 5 to calculate the long term strength as T_{LTDS}=33.84/RF=16.92 kN/m. Running Bishop's analysis for the aforementioned geosynthetic long-term design strength yields *Fs*=1.31. For illustrative purposes, the safety map shown in Fig. 2 was generated using T_{LTDS}=16.0 kN/m, rendering a *Fs* of 1.30, which will henceforth be considered the baseline Stage II safety map for the presented example. It is noted only circular arcs were considered in demonstrating the Stage II analysis; however, it is possible that other failure mechanisms might be more critical and thus need to be considered.

The two stages in design are compatible with current design philosophy, complementing each other. Stage I produces a tension map that demonstrates utility for selecting reinforcement and connection specifications including a factor of safety, $F_{s\text{-}g}$, on reinforcement ultimate strength. Stage II ensures that for the selected reinforcement (with its associated long-term strength and connection capacity), the soil shear strength is adequately mobilized as manifested by a common slope stability factor of safety, *Fs*. Should the computed margin or factor of safety, *Fs*, in Stage II be less than, say, 1.3 (Berg et al. 2009), the strength and/or layout of reinforcement should be adjusted to produce a more optimal design. Such an adjustment can be done effectively and objectively using the safety and tension maps. Examples and details are given in Leshchinsky et al. (2016).

Illustrative Examples

To realize the outcome of the presented framework, a few instructive examples are presented. As a baseline problem, consider the slope geometry, reinforcement layout, and soil data related to Fig. 2. Figs. 5, 7 and 8 show the baseline results.

Fig. 9 shows the distribution of computed loads in the reinforcement considering the impact of small block facing units. The blocks considered are 0.3 m high and 0.3 m deep, having bulk unit weight of γ_u=24 kN/m^3. It is noted that the specified block dimensions are merely for convenience; however, these value do not affect the generality of the conclusions. For design, the block-to-block interface friction is taken as $\delta_{b\text{-}b}$=38 degrees while the bottom block (or leveling pad) and foundation is $\delta_{b\text{-}f}$=28 degrees, same as the strength of the foundation soil. Any 'adhesion' (or interlocking) between blocks is ignored, but can be accounted for if one so chooses. Consideration of this interlocking resistance can have a significant effect on reinforcement mobilization, even realizing scenarios where little or no reinforcement is required. Nonetheless, in this case, the frictional shear force resistance between blocks and between the bottom block (or leveling pad) and foundation are calculated using the weight of column of stacked blocks located above the analyzed interface multiplied by *tan*($\delta_{b\text{-}b}$) or *tan*($\delta_{b\text{-}f}$), respectively. Bishop's equation then is modified to consider mobilized horizontal resisting force at the emerging point where the circle exits the slope. For each analyzed circle, only one such interface is relevant (Leshchinsky et al. 2016).

Comparing Figs. 7 and 9, one can see that the interblock frictional resistance at a limit state notably decreases the reinforcement force near the front end, reducing effective connection loading. In fact, while max(T_{max}) decreases from 11.28 to 10.14

kN/m (about a 10% decrease) due to the facing units, the connection load decreases dramatically to near zero for most layers – Fig. 10. That is, small facing units affect have significant influence on connection loading but have little global effect. This phenomenon is a result of relatively weak interfaces available in narrow, small blocks while considering frictional interface properties only. Upon comparison of Figs. 7 and 9, the inclusion of the aforementioned facing units result in a locus of $T_{\max\text{-}i}$ that is slightly deeper. If one uses interface adhesion of, say, 50 kPa (e.g. representative of an interlocking shear key) at both in between blocks and at the foundation, max(T_{max}) drops to 7.51 kN/m (from 10.14 kN/m), an approximate 25% decrease. Concurrently, the connection loads drop significantly. However, if the interface with the foundation remains with only $\delta_{b\text{-}f}$=28 degrees while blocks to blocks has adhesion of 50 kPa, max(T_{max}) drops to only 9.88 kN/m. The interface with the foundation remains weak thus facilitating preferential emergence of slip surfaces at that location, bypassing stronger interfaces above. The end result then is little reduction in max(T_{max}) value. Note that 'adhesion' due to interlocking should be used with caution as it does not represent plastic or Mohr-Coulomb strength but rather strength of a brittle material. Furthermore, note that the methodology in this paper would demonstrate that increasing block size would eventually render the reinforcement unnecessary, as the wall transitions from a hybrid structure to a gravity wall.

Selection of reinforcement spacing has a profound effect on realized reinforcement loading. The baseline example uses vertical reinforcement spacing of S_v=0.6 m (10 layers) with the bottom layer placed 0.3 m above the foundation. Consider the same problem but with S_v=0.3 m (a total of 19 layers). A comparison of

Figure 11 with Figure 7 (the baseline case) demonstrates a drop in maximum loading and a relatively uniform mobilization of maximum loading – an indicator of a more efficient structure. The value of max(T_{max}) drops from 11.28 kN/m for the baseline problem to 5.65 kN/m for 0.3 m spacing, a 50% drop that is essentially proportional to the spacing. However, there is a dramatic drop in connection load, mainly in upper layers – Fig. 12. While the simple pullout model used in this work (Eq. 2) is unaffected by spacing, the intensity of force distribution in the reinforcement decreases proportionally. Hence, the required tangential translation of the front end pullout envelope rapidly decreases as the spacing gets closer, resulting in concurrent rapid decrease in connection load.

While FHWA guidelines (Berg et al. 2009) (FHWA) consider intermediate or secondary reinforcement layers as a compaction aide next to a steep slope, it does not consider its effects as reinforcement. To explore the impact of intermediate layers, 1.5 m long secondary reinforcements were introduced between the long (4.2 m) primary reinforcement layers used in the baseline problem. The total number of reinforcement layers is 19; however, compared to the closely spaced reinforcement, the quantity of total reinforcement layers used drops by approximately 30%. Fig. 13 shows the impact of intermediate layers. The value of max(T_{max}) drops from 11.28 kN/m for the baseline problem to 7.51 kN/m, a 33% drop. For the closely-spaced case, max(T_{max}) was 5.65 kN/m. Figure 14 shows that for intermediate layers the reduction in connection loading is as effective as when closely-spaced reinforcements are employed. Also, Fig. 14 illustrates the increasingly oscillating values of $T_{\text{max-}i}$ towards the upper portion of the slope. This behavior is due to deeper slip surfaces in that region extending beyond the

effective length of the intermediate layers. However, the effectiveness of these layers in reducing $T_{o\text{-}i}$ is evident all along the height rendering values similar to full-length closely-spaced reinforcement.

Although discussed, Stage II in design is not conducted here for the illustrative example problems. However, as stated before, global stability assessment (Stage II) must be conducted to ascertain that the outcome of Stage I indeed renders an adequate *Fs*.

Concluding Remarks

This study presents a rational LE framework that renders a layer-by-layer, tensile force distribution for any given configuration of reinforcements at a limit state. This distribution is a function of the geometry of the slope, the soils comprising the slope, the layout of the reinforcements, the parameters characterizing the interaction of the reinforcement with the confining soil, and other relevant aspects. The tensile distribution is determined by iteratively assessing slip surfaces at various entrance and exit locations while varying the mobilized force in the reinforcement, aiming to produce the same limit state along each discretized increment of a respective reinforcement layer. That is, this process seeks to represent any point within the reinforced mass with a *SF*=1.0 and hence, the same margin of safety as expressed by *Fs*. The end result of this analysis is the creation of a tension map, which produces the maximum tensile force mobilized in each layer as well as the connection load between the reinforcement and the facing. Based on the demand realized from a tension map, a designer can then select appropriate geosynthetic reinforcements and connection specifications

578 considering reduction factors for installation damage, durability, creep, as well as an
579 applied factor of safety on the long term strength (i.e., standard procedure in selecting
580 geosynthetic reinforcement with adequate ultimate strength). However, while this stage
581 of design ensures 'local' stability considering the reinforcement force as a variable, it
582 may not guarantee global stability where the soil strength mobilized is limited by a
583 prescribed, minimum factor of safety (e.g., $Fs \geq 1.3$). Hence, after selecting the
584 reinforcement based on the first stage, the designer needs to conduct a conventional LE
585 stability assessment in the second stage. Compound and foundation/deep-seated
586 failures need to be assessed while the reinforcement strength is limited by its *actual*
587 long term strength. This strength is *not* subjected to an *additional* factor of safety ($F_{s\text{-}g}$)
588 since the target global factor of safety, *Fs*, *de facto* considers 'weaker' soil and
589 therefore, results in stronger and longer reinforcement than needed for actual limit state.
590 This long term strength along the reinforcement is limited by pullout resistance at the
591 rear and front ends of each reinforcement layer. After pullout resistance at the rear of
592 the reinforcement provides an envelope for allowable loading, connection load is
593 similarly used to ascertain that sufficient front end pullout capacity exists.

594 Stage I is a rational and robust alternative to conventional internal stability design
595 which is based on lateral earth pressures. It can deal seamlessly with reinforced slopes
596 and walls. It serves to select the reinforcement and connectors considering local
597 conditions anywhere within the soil mass. Stage II ensures global stability considering
598 the long-term strength of the reinforcement and connection. Use of Stage II after
599 conducting Stage I prevents the possibility of locally overstressing a reinforcement
600 layer. Furthermore, use of $Fs > 1.0$ in Stage II will render a system at working load

conditions; i.e., a system that has a prescribed margin of safety against mobilization of the soil's full strength.

Examples show that closely-spaced reinforcement decrease the reinforcement load proportional to spacing while disproportionally and possibly dramatically decreasing the connection loads. Intermediate or secondary layers are also effective in decreasing the connection load while reducing max(T_{max}). Facing units may also decrease the connection loading. For the baseline case, which is comparable with AASHTO, the reinforcement strength required using the LE framework is about half that computed using the AASHTO method.

Generally, the connection loads, $T_{o\text{-}i}$, produced by the LE framework at a limit state are small relative to AASHTO's design method. However, the connection load at the top layer could be large, especially if the spacing or backslope is large. The following comments are made:

1. The LE methodology is herein applied to an entire structure after complete construction. However, during construction, as layers are placed sequentially, each layer will serve temporarily as a 'top' layer. Hence, the *short term* connection load for each layer below the final top layer could exceed the connection load at the top, even if for the final structure the load at the lower connections decrease. This aspect should be considered in the short term strength of the connection.

2. $T_{o\text{-}i}$ was obtained for limit state where some facing movement, mainly during construction, is acceptable. However, this may cause a serviceability issue in critical applications such as bridge abutments or in cases where footings of buildings are located over the reinforced soil zone. That is, when high surcharge is applied after

construction is complete. In such cases one may require that the connection capacity at each elevation be equal to the limit state maximum load in the respective reinforcement layer; i.e., $(T_{o\text{-}i})_{imposed} = T_{max\text{-}i}$. Fig. 15 schematically shows this imposed requirement. However, one must be wary of parasitic loading stemming from differential settlement between the facing elements and backfill, which can induce connection forces that are not easily quantified.

3. Regardless of serviceability considerations mentioned in comment (2), firmly restraining the facing through increased connection capacity (Fig. 15) should result in the following:

   – Better compaction next to the facing, an important element responsible for good performance of earth structures.

   – Better confinement at the facing. Such confinement stiffens the reinforced soil mass as well as increase the soil strength, resulting in additional margin of safety for stability.

   In lieu of firmly restraining the facing (i.e., use T_o for limit state rather than T_o=T_{max} as in Fig. 15), closely-spaced reinforcements combined with high-quality compacted backfill can be used. The restraining behavior and confinement produced by such a technique has a proven record in numerous constructed GRS walls.

Generally, performance of most MSE structures is not sensitive to minor movements of the facing. Furthermore, experience indicates that in many systems with moderate connection capacity, such as block walls with frictional connection, existing construction techniques ensure acceptable overall performance. Consequently, long term connection

capacities implied by the LE framework, especially for closely-spaced reinforcements, are adequate provided that Comment (1) is satisfied.

Finally, the presented framework within this study is novel, but the present implications of its application through a series of rigorous examples are incomplete. A more robust collection of additional example problems, computational details, comparisons with experimental and numerical results, and use of LE in design codes, are provided in Leshchinsky et al. (2016, 2017a, 2017b). Future modifications could account for various failure kinematics, facing details and MSE or GRS systems.

References

AASHTO. (2012). Standard specifications for highway bridges. 17th edition. American Association of State Highway and Transportation Officials (AASHTO), Washington, D.C.

Baker, R., and Klein, Y. _2004a_. "An integrated limiting equilibrium approach for design of reinforced soil retaining structures: Part I—Formulation." *Geotext. Geomembr.*, 22_3_, 119–150.

Baker, R., and Klein, Y. _2004b_. "An integrated limiting equilibrium approach for design of reinforced soil retaining structures: Part II— Design examples." *Geotext. Geomembr.*, 22_3_, 151–177.

Berg, R., Christopher, B.R., and Samtani, N., (2009). *Design of mechanically stabilized earth walls and reinforced soil slopes*, Vols. I and II, Reports No. FHWA-NHI-10-024/025, Federal Highway Administration, 684 pp.

Duncan, J. M. (1996). State of the art: limit equilibrium and finite-element analysis of slopes. *Journal of Geotechnical engineering*, *122*(7), 577-596.

Leshchinsky, D., Leshchinsky, O. and B. Leshchinsky. (2017a). Part 1: 'Geosynthetic reinforced soil 101' leading to rational design of MSE walls and slopes. *Geosynthetics Magazine April-May 2017, 24-31.*

Leshchinsky, D., Leshchinsky, O. and B. Leshchinsky. (2017b). Part 2: 'Geosynthetic reinforced soil 101' leading to rational design of MSE walls and slopes. *Geosynthetics Magazine June-July 2017, 22-28.*

Leshchinsky, D., Leshchinsky, O., Zelenko, B., & Horne, J. (2016). *Limit Equilibrium Design Framework for MSE Structures with Extensible Reinforcement* (No. FHWA-HIF-17-004).

Leshchinsky, D. _1992_. "Issues in geosynthetic-reinforced soil." Keynote paper, *Proc., Int. Symp. Earth Reinforcement Practice*, Vol. 2, Kyushu, Japan, Balkema, Rotterdam, The Netherlands, 871–897.

Leshchinsky, D. and Boedeker, R. H., (1989). "Geosynthetic Reinforced Soil Structures," *Journal of Geotechnical Engineering*, ASCE, 115(10), 1459-1478.

Leshchinsky, D. and Han, J., 2004. "Geosynthetic Reinforced Multitiered Walls," ASCE, *Journal of Geotechnical and Geoenvironmental Engineering,* 130(12), 1225-1235.

Leshchinsky, D. and Reinschmidt, A.J., (1985). "Stability of Membrane Reinforced Slopes," *Journal of Geotechnical Engineering*, ASCE, 111(11), 1285-1300.

Leshchinsky, D., & Vulova, C. (2001). Numerical investigation of the effects of geosynthetic spacing on failure mechanisms in MSE block walls. *Geosynthetics International*, *8*(4), 343-365.

Leshchinsky, D., Kang, B., Han, J., & Ling, H. (2014). Framework for limit state design of geosynthetic-reinforced walls and slopes. *Transportation Infrastructure Geotechnology*, *1*(2), 129-164.

Leshchinsky, D., Ling, H.I. and Hanks, G., (1995). "Unified Design Approach to Geosynthetic Reinforced Slopes and Segmental Walls," *Geosynthetics International*, 2(4), 845-881.

Liu, H. (2016). Required reinforcement stiffness for vertical geosynthetic-reinforced-soil walls at strength limit state. *Géotechnique*, *66*(5), 424-434.

Mohamed, S. B., Yang, K. H., & Hung, W. Y. (2014). Finite element analyses of two-tier geosynthetic-reinforced soil walls: comparison involving centrifuge tests and limit equilibrium results. *Computers and Geotechnics*, *61*, 67-84.

National Concrete Masonry Association (NCMA). (1997). Design manual for segmental retaining walls, 2nd edition, J.G.Collin, ed., National Concrete Masonry Association, Herndon, Va.

Rowe, R. K., and Ho, S. K. _1992_. “A review of the behavior of reinforced walls.” Keynote paper, *Proc., Int. Symp. on Earth Reinforcement Practice*, Vol. 2, Kyushu, Japan, Balkema, Rotterdam, The Netherlands, 801–830.

Smith, C. C., & Tatari, A. (2016). Limit analysis of reinforced embankments on soft soil. *Geotextiles and Geomembranes*, *44*(4), 504-514.

Wright, S. G., & Duncan, J. M. (1991). Limit equilibrium stability analyses for reinforced slopes. *Transportation Research Record*, (1330).

Xie, Y., & Leshchinsky, B. (2015). MSE walls as bridge abutments: Optimal reinforcement density. *Geotextiles and Geomembranes*, *43*(2), 128-138.

Figure Caption List

Figure 1. Available tensile resistance along reinforcement in current design.

Figure 2. (a) Bishop's method of slope stability applied to reinforced soil; (b) Example problem: Safety map using Bishop Method.

Figure 3. Flow chart representing the steps of the Top-Down procedure.

Figure 4. Schematic of the iterative calculation of reinforcement tensions applied by the Top-Down procedure.

Figure 5. (a) Computed load distribution in top 3 layers, constrained by rear end pullout resistance, considering load shedding amongst layers. (b) Load distribution in all 10 layers superimposed by rear end pullout resistance.

Figure 6. Determination of connection load by shifting front end pullout to be tangent to the distribution of force in reinforcement for (a) top layer and (b) bottom layer.

Figure 7. Locus of $T_{max\text{-}i}$ superimposed on force distribution along each reinforcement.

Figure 8. Calculated baseline data: $T_{max\text{-}i}$ and $T_{o\text{-}i}$ using LE and AASHTO (2002).

Figure 9. Effects of facing on force distribution in reinforcement (black squares represent the locus of $T_{max\text{-}i}$)

Figure 10. Comparison of the influence of facing elements on reinforcement loading.

Figure 11. Effects of close spacing on force distribution in reinforcement (black squares represent the locus of $T_{max\text{-}i}$)

Figure 12. Comparison of the influence of reinforcement vertical spacing on loading.

Figure 13. Effects of intermediate layers on force distribution in reinforcement (black squares represent the locus of $T_{max\text{-}i}$).

Figure 14. Calculated $T_{max\text{-}i}$ and $T_{o\text{-}i}$ in consideration of secondary reinforcement layers.

Figure 15. Link between LE results and possible design specifications.

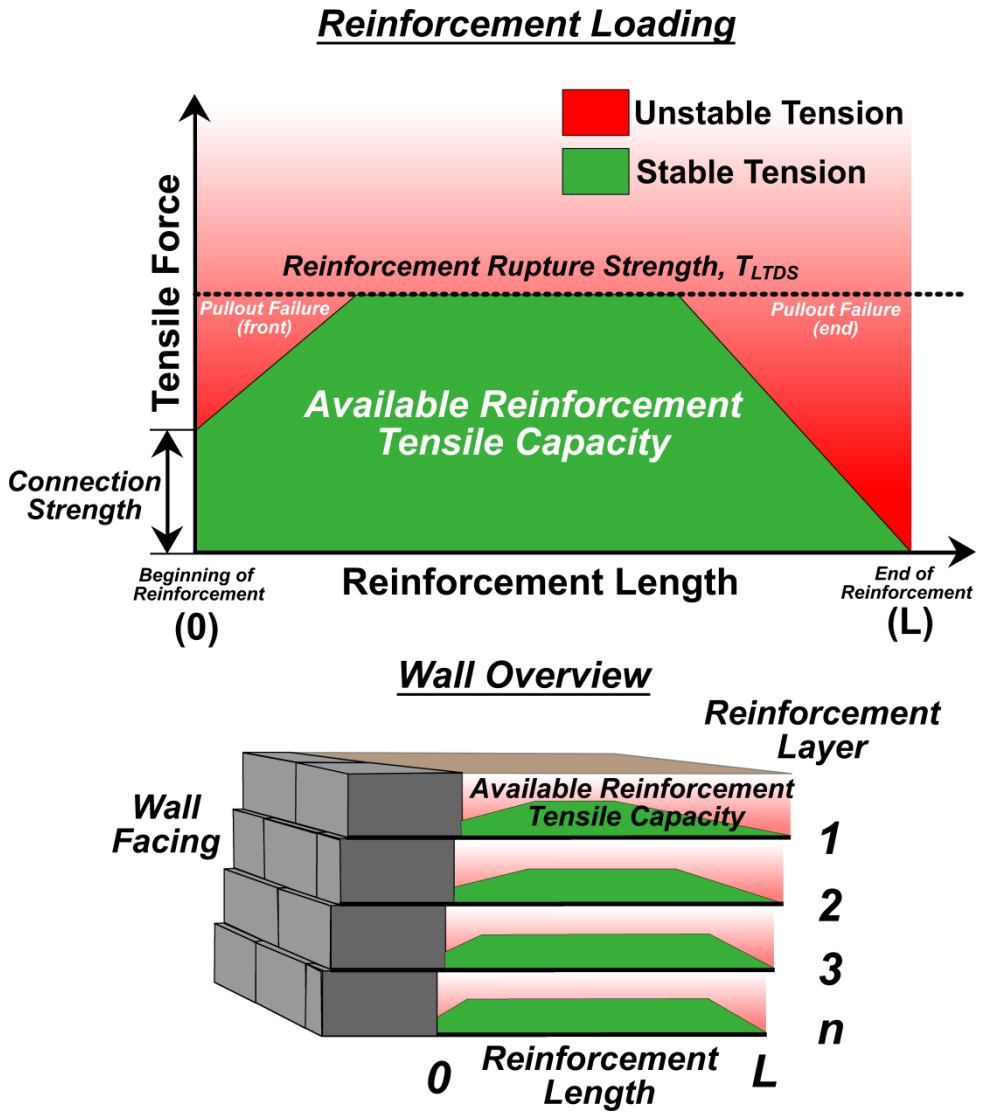

734

735 **Figure 1.** Available tensile resistance along reinforcement in current design.

736

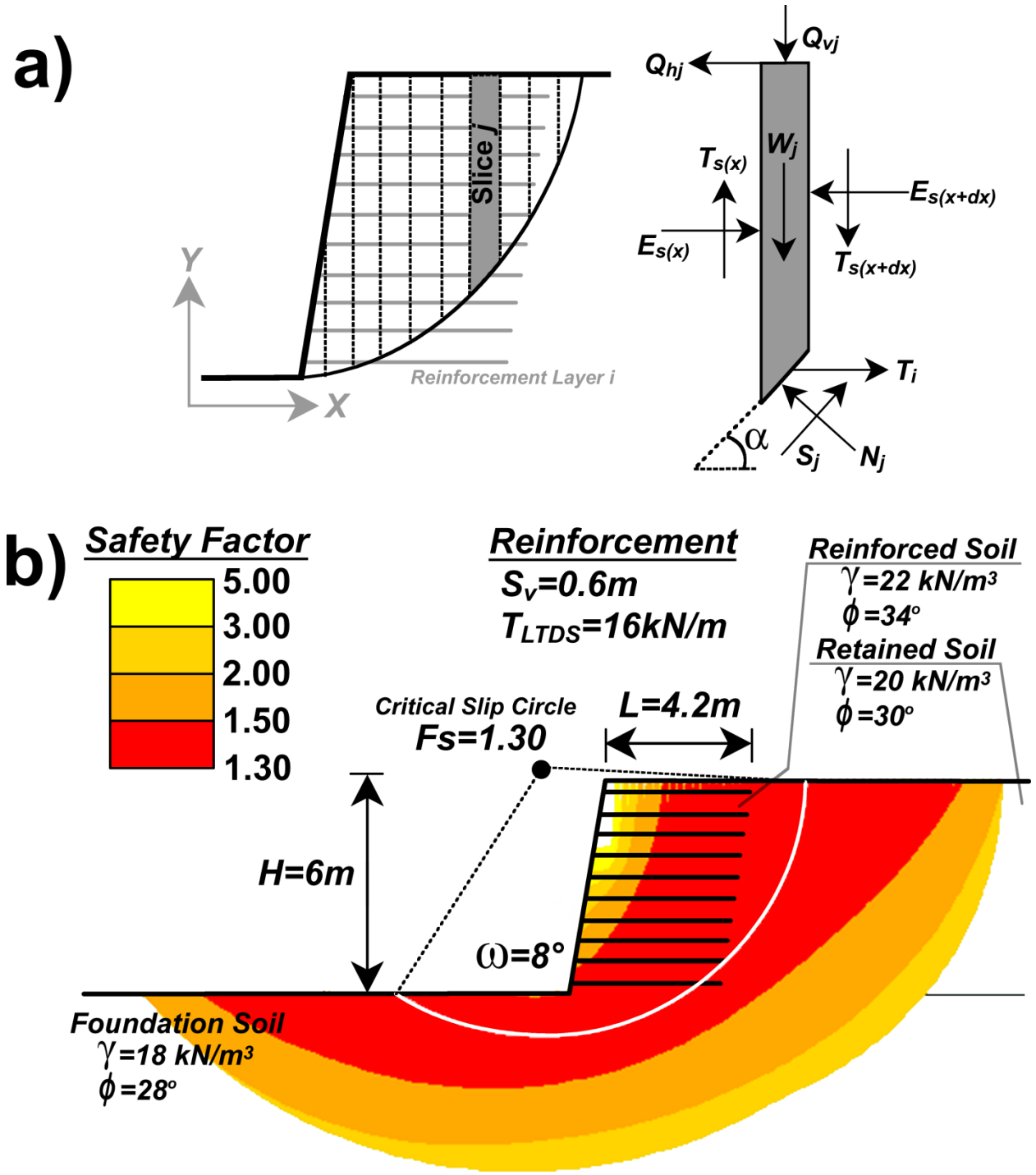

737

738 **Figure 2.** (a) Bishop's method of slope stability applied to reinforced soil; (b) Example

739 problem: Safety map using Bishop Method.

740

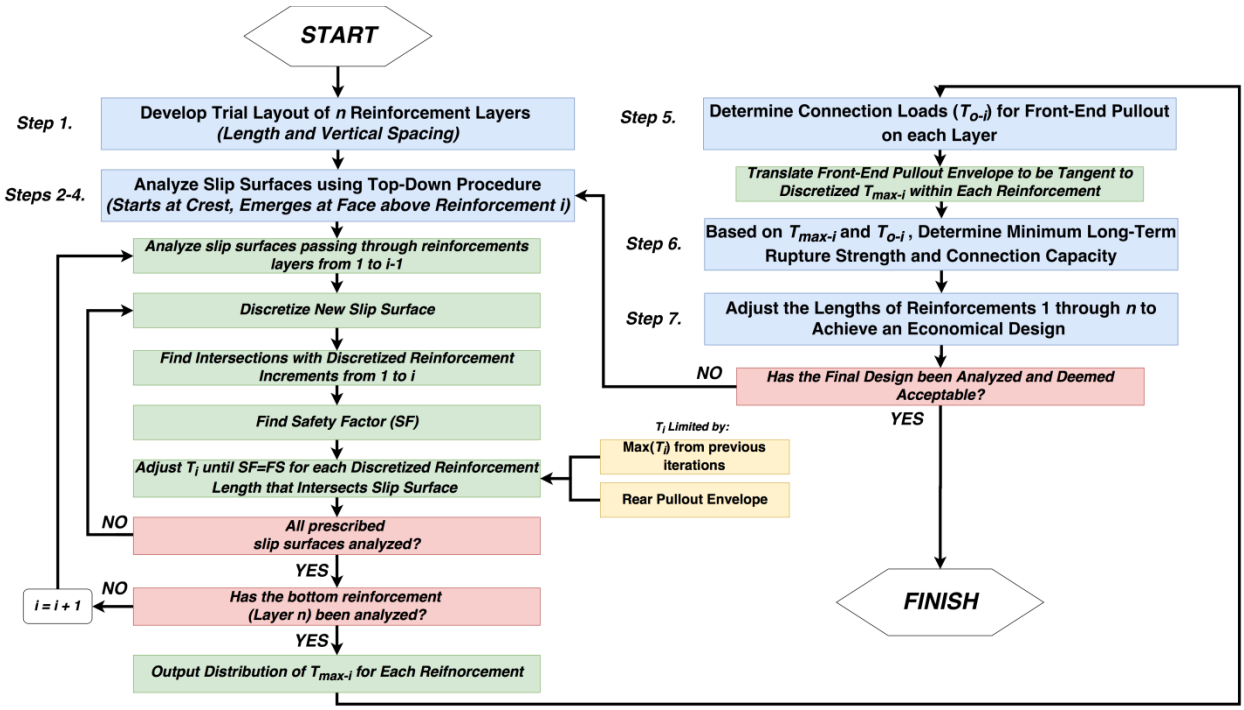

741

742 **Figure 3**. Flow chart representing the steps of the Top-Down procedure.

743

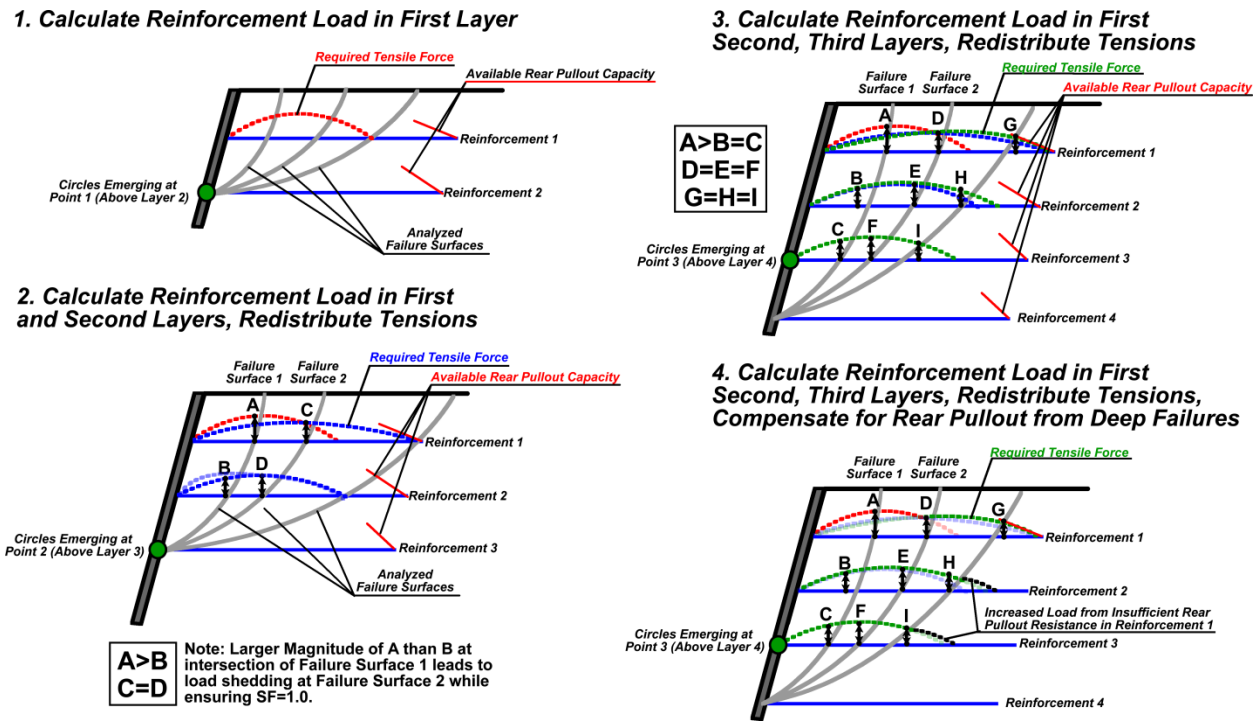

744

745 **Figure 4.** Schematic of the iterative calculation of reinforcement tensions applied by the
746 Top-Down procedure.

747

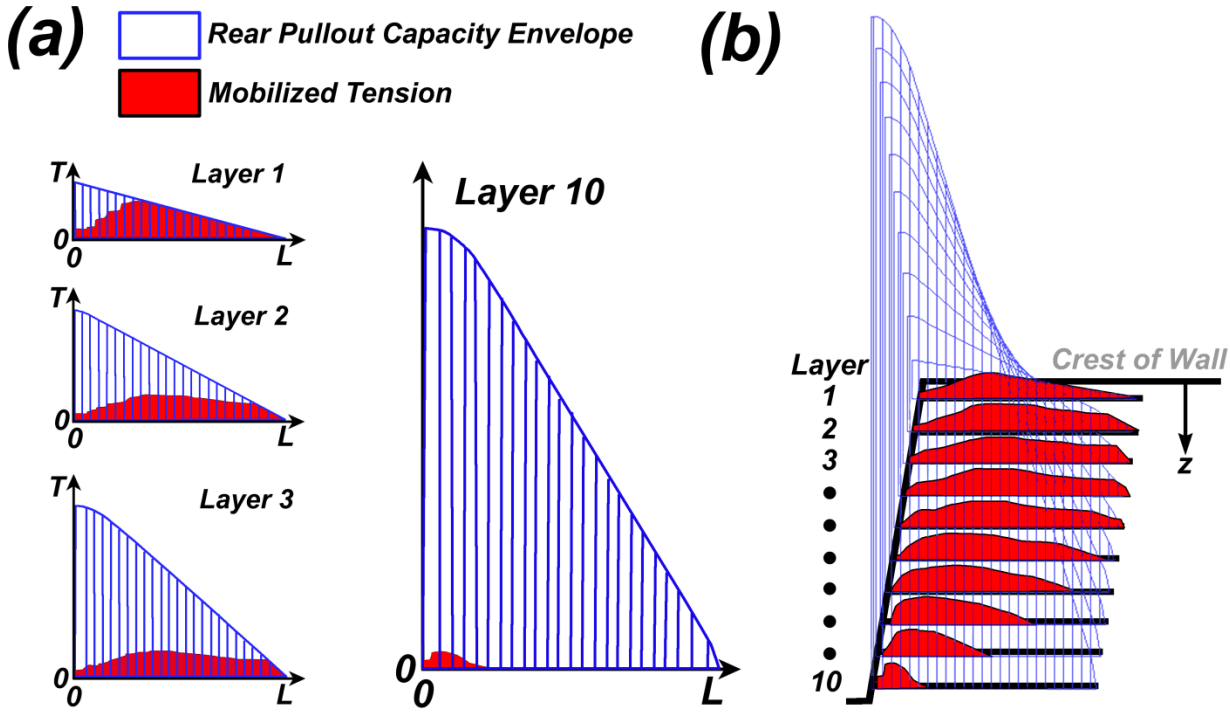

Figure 3. (a) Computed load distribution in top 3 layers, constrained by rear end pullout resistance, considering load shedding amongst layers. (b) Load distribution in all 10 layers superimposed by rear end pullout resistance.

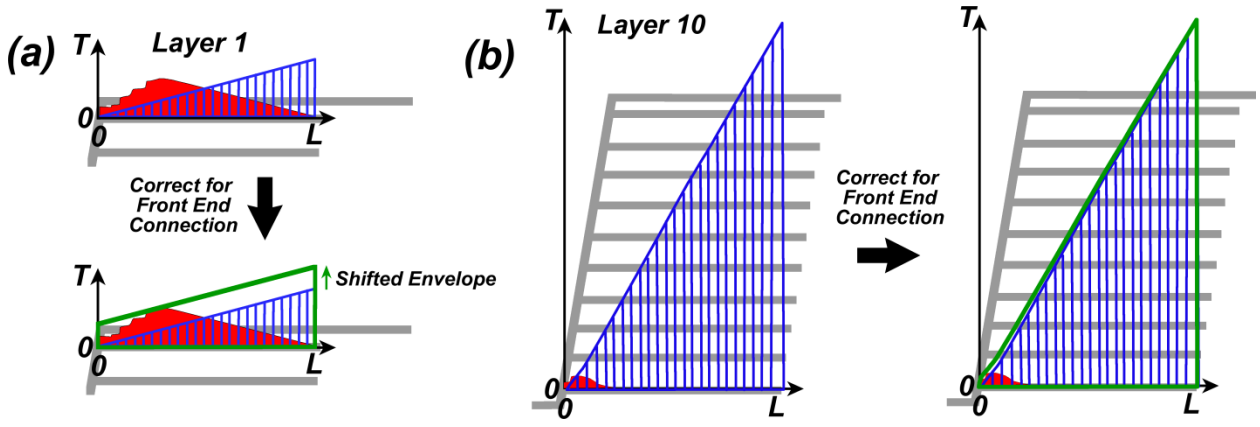

Figure 4. Determination of connection load by shifting front end pullout to be tangent to the distribution of force in reinforcement for (a) top layer and (b) bottom layer.

760

761

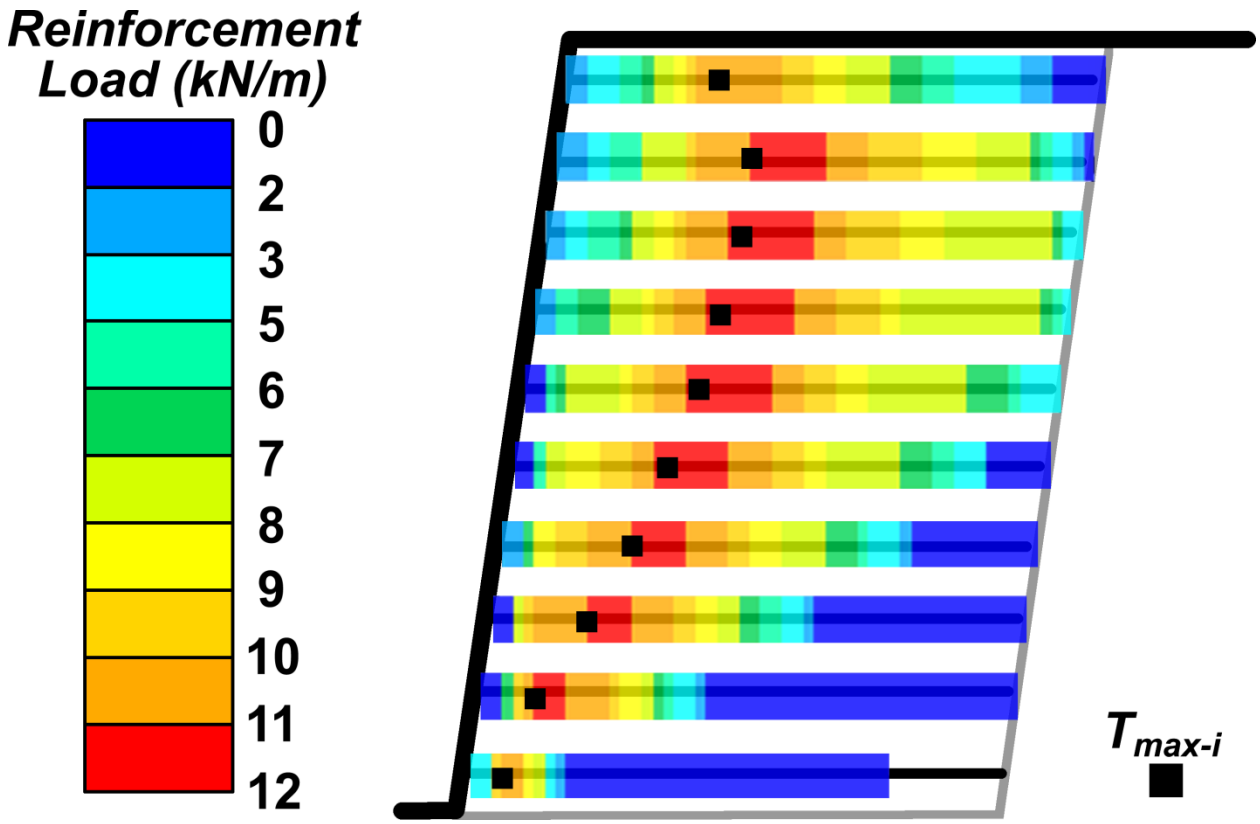

762

763 **Figure 5.** Locus of T_{max-i} superimposed on force distribution along each reinforcement.

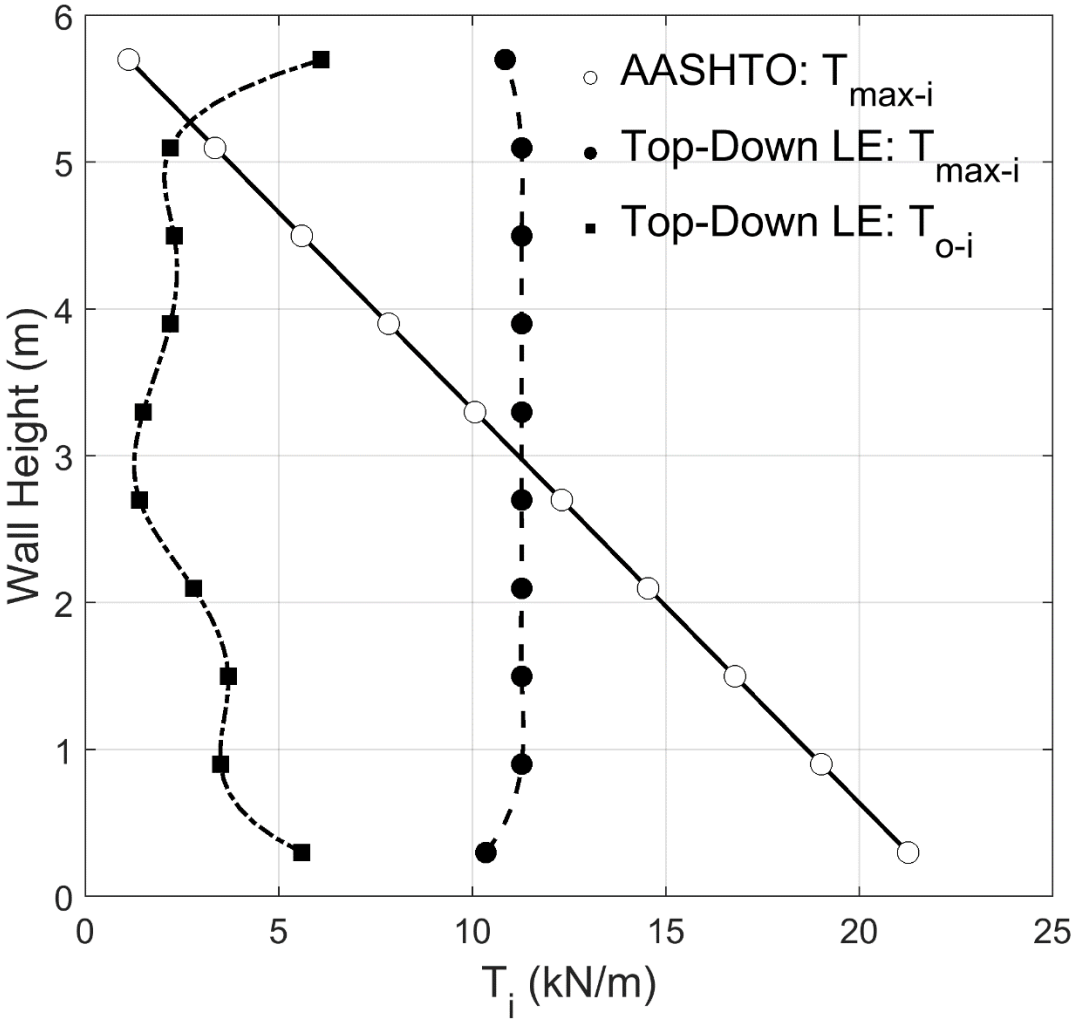

764

765 **Figure 6.** Calculated baseline data: $T_{max\text{-}i}$ and $T_{o\text{-}i}$ using LE and AASHTO (2002).

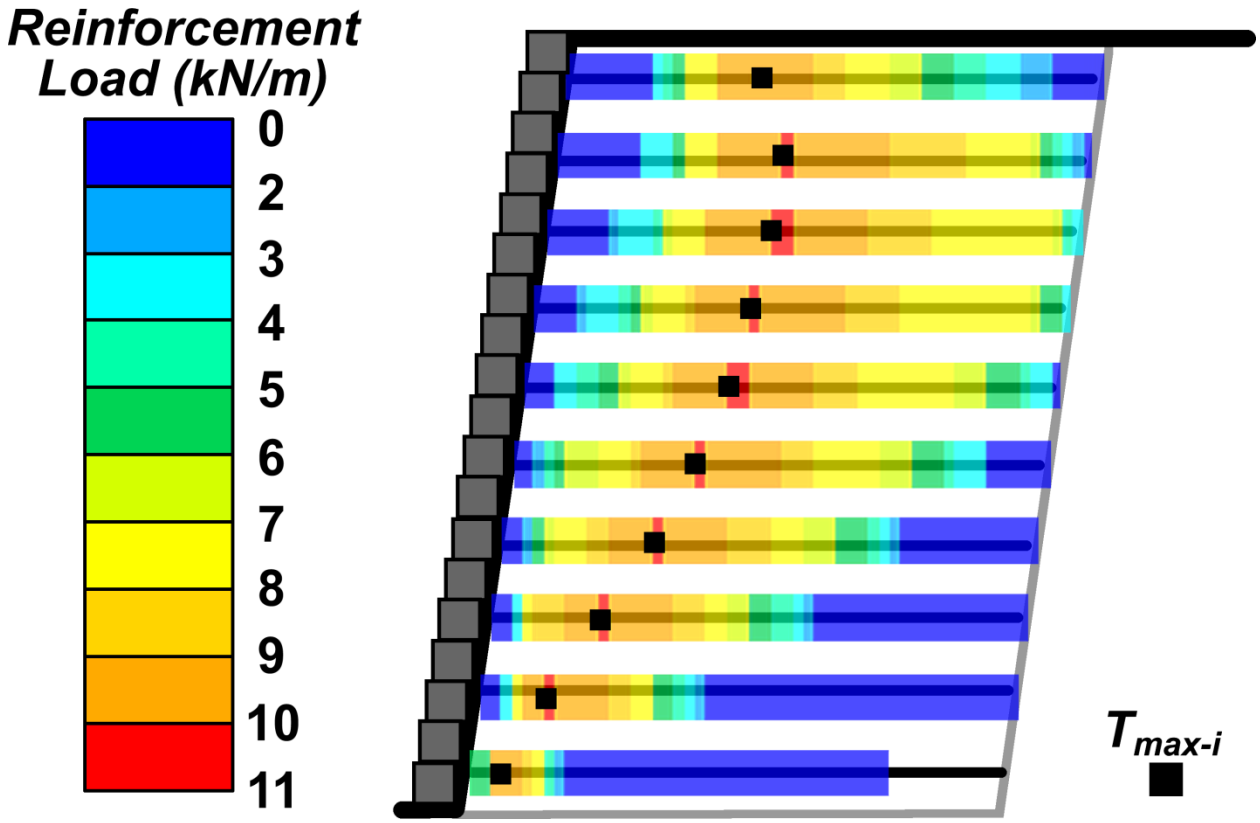

766

767 **Figure 7.** Effects of facing on force distribution in reinforcement (black squares

768 represent the locus of T_{max-i})

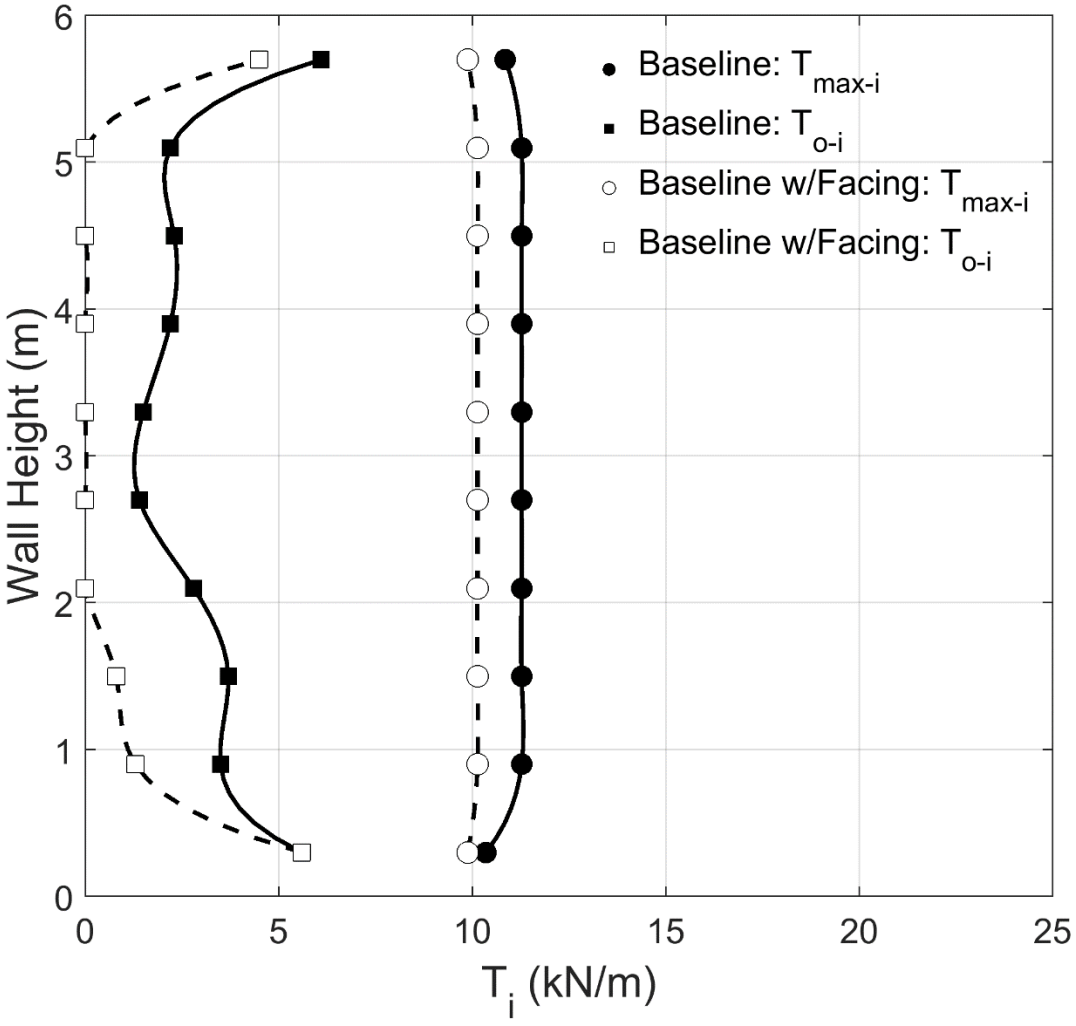

769

770 **Figure 8.** Comparison of the influence of facing elements on reinforcement loading.

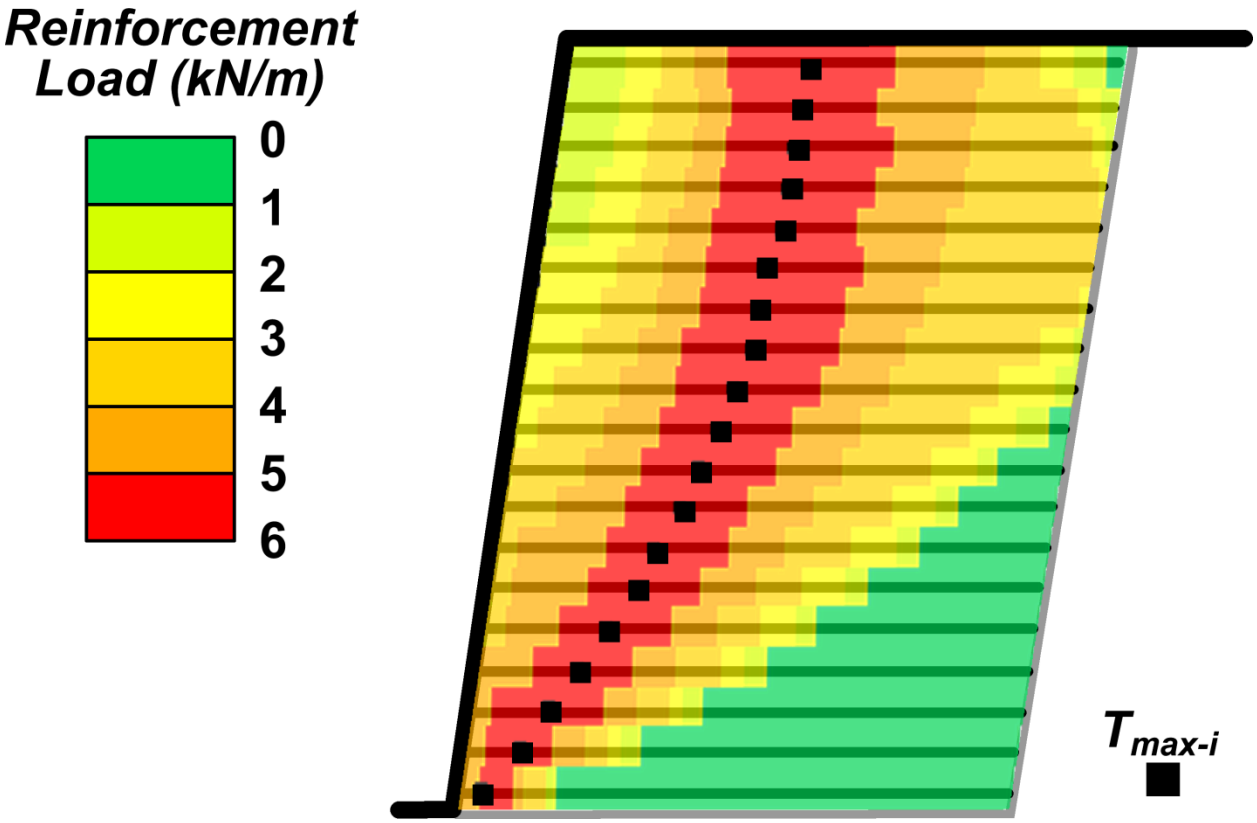

771

772 **Figure 9.** Effects of close spacing on force distribution in reinforcement (black squares

773 represent the locus of $T_{max\text{-}i}$)

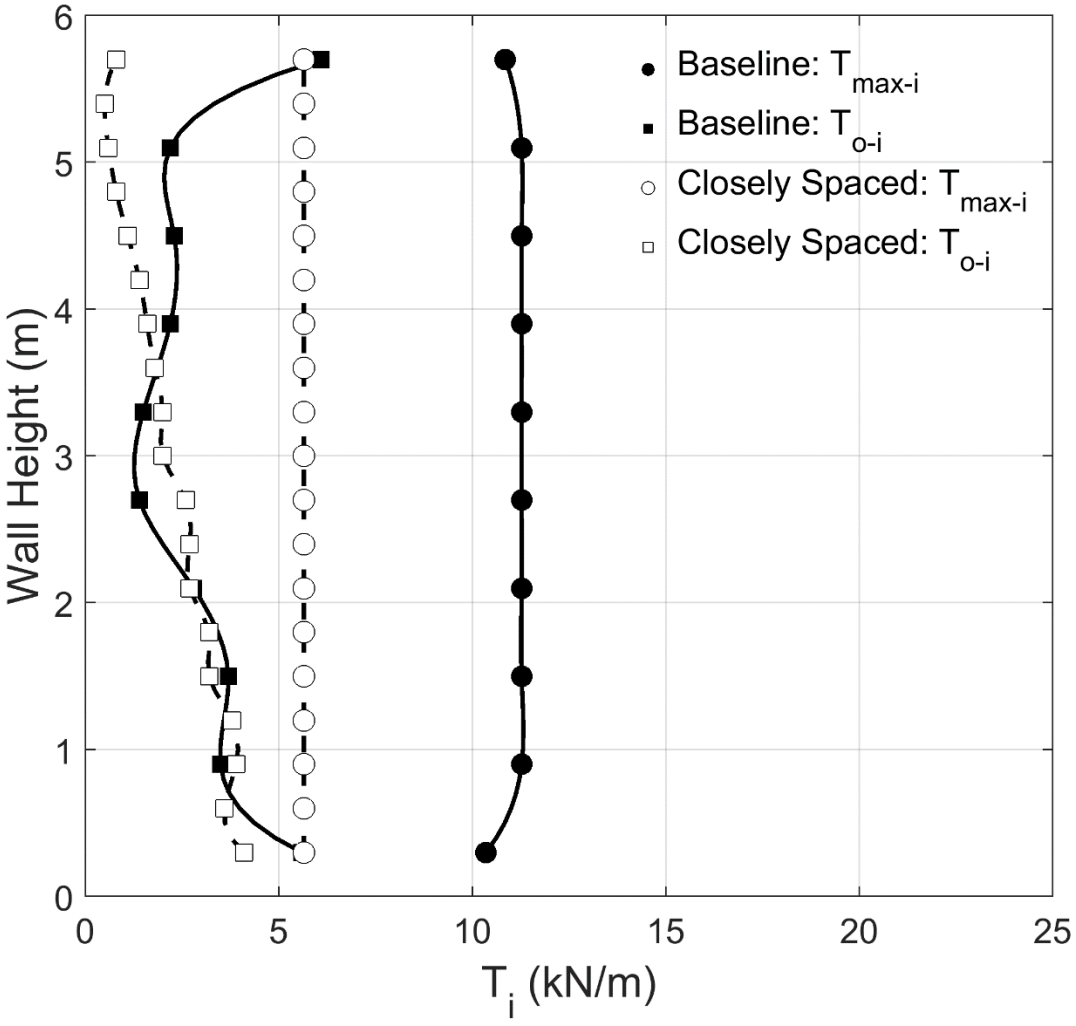

774

775 **Figure 10.** Comparison of the influence of reinforcement vertical spacing on loading.

776

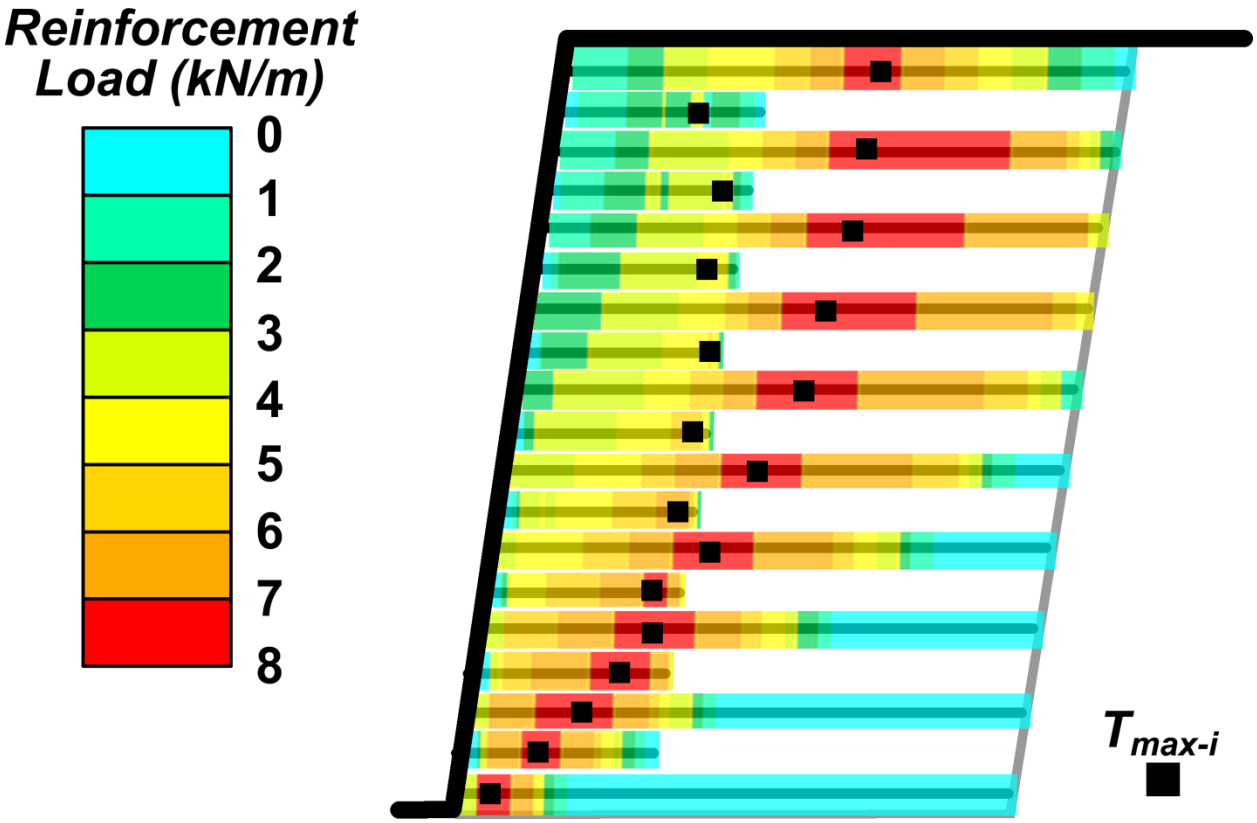

777

778 **Figure 11.** Effects of intermediate layers on force distribution in reinforcement (black

779 squares represent the locus of $T_{max\text{-}i}$).

780

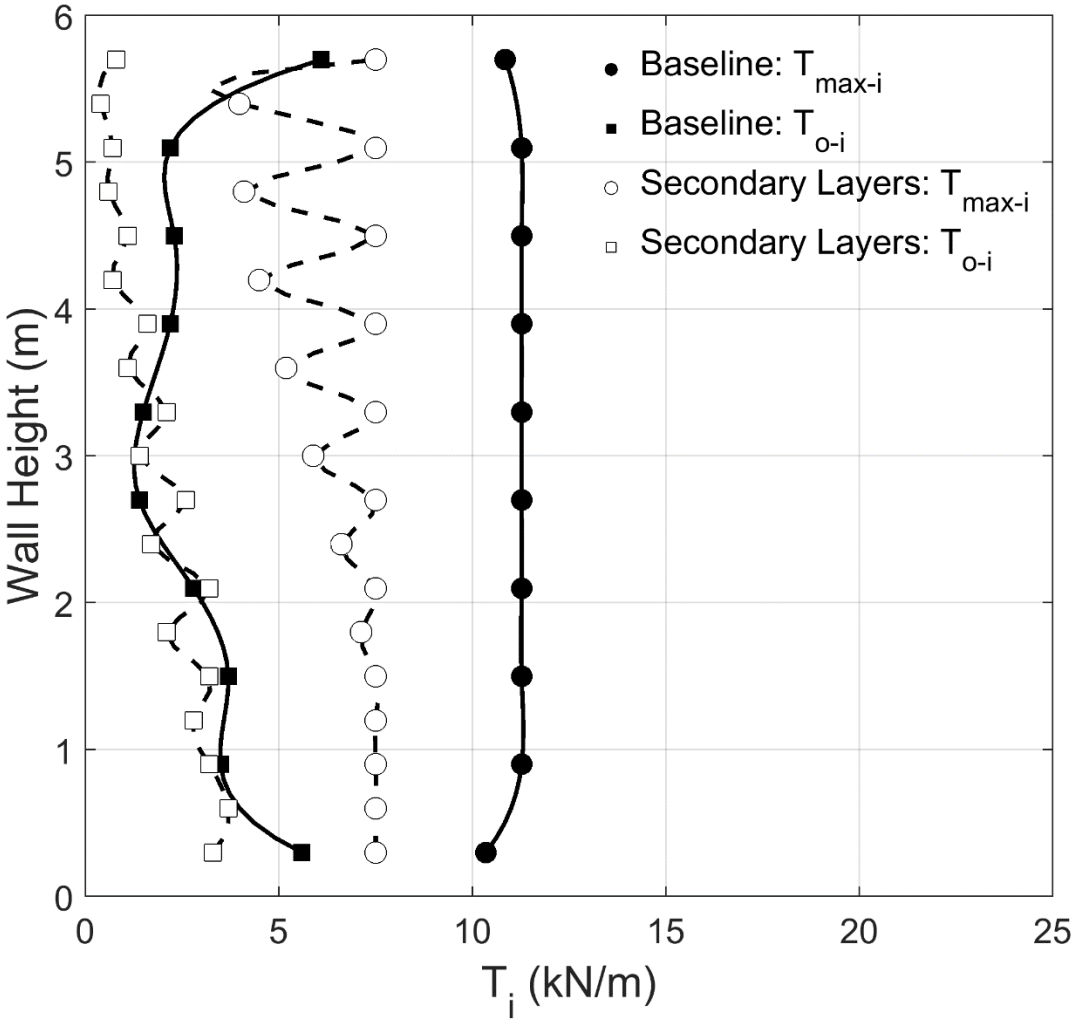

781

782 **Figure 12.** Calculated $T_{max\text{-}i}$ and $T_{o\text{-}i}$ in consideration of secondary reinforcement layers.

783

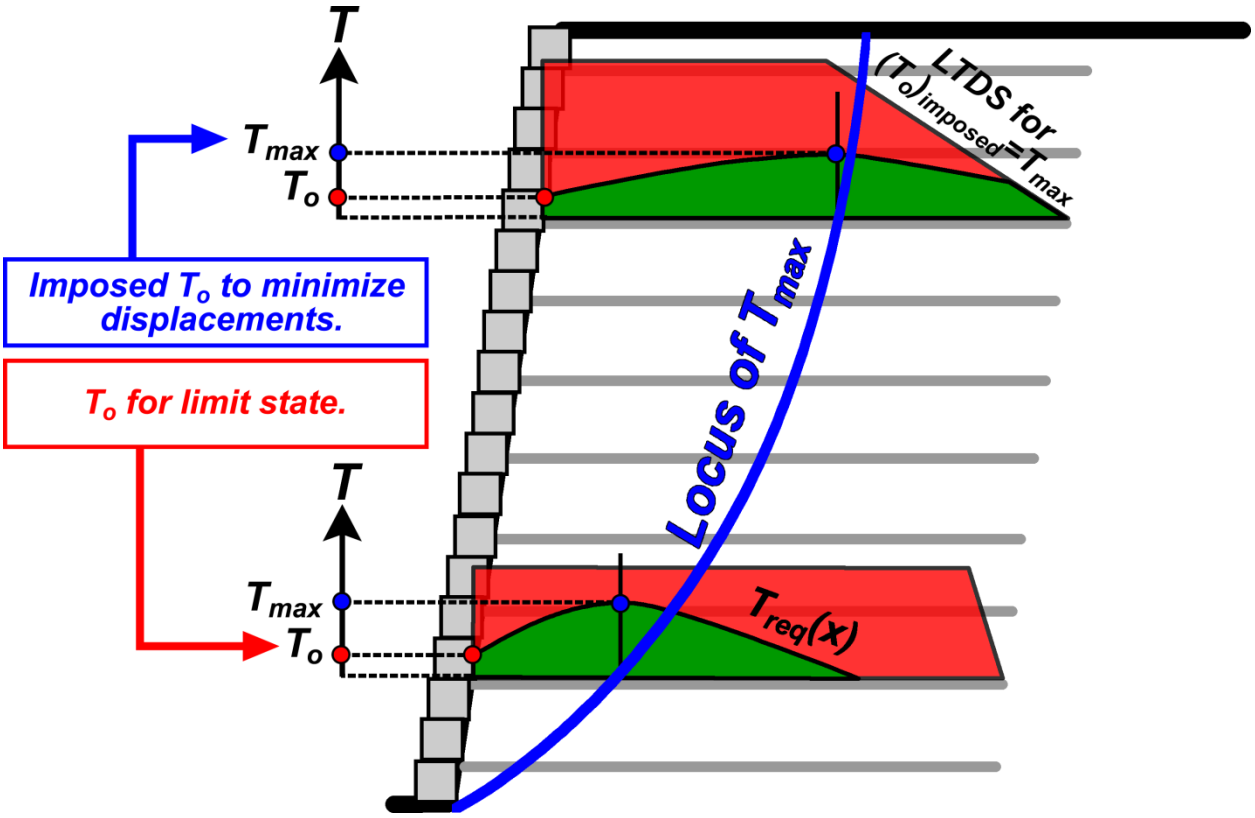

Figure 13. Link between LE results and possible design specifications.